Volume 306, number 2,3, 234–238 FEBS 11299 July 1992

Computational approach towards the three-dimensional structure of *E. coli* tyrosine aminotransferase

J. Jäger[1], T. Solmajer[2] and J.N. Jansonius

Biozentrum der Universität Basel, Klingelbergstr. 70, CH-4056 Basel, Switzerland

Received 13 May 1992

We present a new model for *E. coli* tyrosine aminotransferase based on the X-ray structures of the wild type and Val[39]Leu mutant of *E. coli* aspartate aminotransferase and computer simulation studies. Active site characteristics of the model are correlated with experimental observations on the specificity of these enzymes towards aromatic/dicarboxylic acid substrates.

Tyrosine aminotransferase; Computer modelling; X-ray structure; Aspartate aminotransferase; Mutant enzyme; *E. coli*

1. INTRODUCTION

Aspartate aminotransferase (AspAT) is one of the most thoroughly studied vitamin B_6-dependent enzymes [1,2]. It catalyzes the reaction:

L-aspartate + 2-oxoglutarate ↔ oxaloacetate + L-glutamate

This transamination reaction is a two-step process in which in step 1 an L-amino acid and water react with the pyridoxal-5′-phosphate (PLP)-enzyme to form a keto acid and the pyridoxamine-5′-phosphate(PMP)-enzyme. In step 2, a second keto acid reacts with the PMP enzyme to give the corresponding L-amino acid and water. In the last decade, several aspartate aminotransferases have been successfully crystallized and subjected to X-ray crystallographic studies. These investigations together with a variety of experimental spectroscopic and biochemical data served as a basis for a detailed structurally based mechanistic proposal [3,4].

The primary structures of a large number of aminotransferases have been determined and compiled [5]. Based on criteria such as substrate specificity, subunit molecular weights and quaternary structures, over 50 distinct enzymes of this family have been identified from eukaryotic and prokaryotic sources. The *E. coli tyrB* gene that encodes another member of the transaminase family, tyrosine aminotransferase (eTyrAT), has been cloned [6] and the protein has been overexpressed. The enzyme was characterized biochemically and was studied by site-directed mutagenesis to probe structure–function relationships [7]. eTyrAT efficiently catalyzes the conversion not only of tyrosine and other aromatic but also of the dicarboxylate substrates. How both dicarboxylic and aromatic substrates are able to bind to the active site of eTyrAT in a productive way is still not well understood. Unfortunately, crystallization experiments in this laboratory with eTyrAT have not been successful to date, precluding crystallographic analyses.

It is evident from primary structure comparisons of eAspAT and eTyrAT that these enzymes, which have a sequence identity of 42.9% (similarity including conservative exchanges: 63%) share catalytically and structurally important residues. The active site region displays a sequence identity of approximately 85%. Using the backbone fold of chicken mitochondrial AspAT in the closed conformation [4], Seville et al. [8] showed that a stereochemically plausible model of eTyrAT can be built, requiring only minor changes in the positions of the main-chain atoms of mAspAT. The study proposed a number of residues as possible determinants of specificity for aromatic substrates. Based on this proposal, several point mutants of eAspAT have been constructed [7,9] in which active site residues found in eTyrAT have been introduced ('hybrid active site' mutants). The mutants have been characterized biochemically and the spatial structures of the wild type and mutant V39L eAspAT have been determined [10–12]. In this work we present a new model for eTyrAT based on the results

Abbreviations: mAspAT, mitochondrial aspartate aminotransferase; eTyrAT, *E. coli* tyrosine aminotransferase; cAspAT, cytosolic aspartate aminotransferase; eAspAT, *E. coli* aspartate aminotransferase; PLP, pyridoxal-5′-phosphate; PMP, pyridoxamine-5′-phosphate; r.m.s., root mean square.

[1]*Present address:* Dept. of Molecular Biophysics and Biochemistry, Yale University, New Haven, CT 06511, USA.
[2]On leave of absence from Institute of Chemistry, P.O.B. 30, 61115 Ljubljana, Slovenia.

Correspondence address: J.N. Jansonius, Dept. of Structural Biology, Biocenter, University of Basel, Klingelbergstr. 70, 4056 Basel, Switzerland. Fax: (41) (61) 267-2109.

 Published by Elsevier Science Publishers B.V.

of the X-ray structure determination of an eAspAT active site mutant with Val^{39} replaced by Leu and on computer simulation experiments. It is expected that such a model would be closer to the true structure than the previous one [8], since the bacterial enzyme eTyrAT is more closely related to the previously unknown structure of eAspAT than to chicken mAspAT. Furthermore, recent advances in computational methods were used to improve the modelling procedure. The revised eTyrAT structure presented herein should be useful for analyzing the determinants of enzyme specificity towards aromatic or dicarboxylic acid substrates.

2. MATERIALS AND METHODS

2.1. *Crystal structure determination*

Crystals of the V39L mutant of *E. coli* AspAT were grown in the presence of the competitive inhibitor maleate at pH 7.5 by the hanging drop method in space group $P2_1$ [10]. Data to 2.5 Å resolution were collected with a FAST (Enraf-Nonius, Delft, Holland) area detector. The structure was solved by molecular replacement, taking initial phases from the model of Seville et al. [8], and refined to a final crystallographic R-factor 0.20 using XPLOR [13]. Maleate was bound in the active site as a Michaelis-type inhibitor. Further details are described elsewhere ([11] and J. Jäger et al., unpublished).

2.2. *Sequence alignments and secondary structure prediction*

Pairwise alignments of the eTyrAT amino acid sequence to a group of AspAT sequences, comprising chicken mAspAT, chicken cAspAT and eAspAT, were performed using the program BESTFIT [14]. Optimal alignments between two sequences were found by inserting gaps to maximize the number of matches using the local homology algorithm of Smith and Waterman [15]. Prediction of secondary structural elements was also carried out in an effort to obtain additional restraints for the molecular dynamics calculations (see below) using both the method of Chou and Fasman [16] and a slightly modified method of Robson-Garnier [17].

2.3. *Model building and computer simulation*

The refined coordinates of the V39L:maleate complex (see above) served as initial template for the modelling of eTyrAT. All eAspAT side chains that differ from the eTyrAT amino acid sequence were exchanged while maintaining the backbone torsion angles. The structure includes a tyrosine residue modelled as a Michaelis complex into the substrate binding site. The substrate α-amino group and the α-carboxylate group have been modelled in accordance with various maleate and 2-methylaspartate complex crystal structures of eAspAT refined at resolutions between 2.3 Å and 2.8 Å [10,12]. These ligands form stable complexes mimicking the Michaelis complex with substrate and the external aldimine reaction intermediate, respectively. The preliminary model was subjected to 300 steps of energy minimization using the XPLOR empirical force field [13]. A harmonic potential of 50 kcal/mol was used to restrain the C_α atoms of the model to their initial positions. Using the program GROMOS [18] a molecular dynamics (MD) simulation at 600K was run for 50 ps to sample the conformational space around the energy minimized structure. The structure was subsequently averaged over the last 30 ps and minimized again. Due to the large size of the system the simulations were carried out in vacuo with a screened Coulombic potential form of nonbonding interactions description [19] as implemented in the program GROMOS. This approach has been shown to yield trajectories, averaged structures, and hydrogen bonding patterns that compare favourably with those calculated for protein systems with explicitly included water, while saving substantial amounts of computer time. In order to utilize the putative secondary structure similarity between eAspAT and eTyrAT, the backbone atoms that were predicted to be part of secondary structural elements in the eTyrAT model structure equivalent to those in the experimental eAspAT structure were also restrained with a harmonic potential of 50 kcal/mol.

3. RESULTS AND DISCUSSION

3.1. *Overall structure and domain organization of eTyrAT*

Inspection of the final model showed that the overall structure, the domain organization, the topology of the large pleated sheet and the locations of all α-helices within the structure remain the same as in the wild type and V39L eAspATs (Fig. 1). Superposition of all equivalent C_α atoms of single eAspAT and eTyrAT subunits (residues 5–409)† gave an r.m.s. deviation of 1.29 Å. Larger displacements are observed mainly in loop regions at the surface of the new eTyrAT model. Residues 27–29, 42–45, 64–67, 120–134, 233, 336–355 and 384–396 show displacements exceeding 2.5 Å. Residue 65 is an insertion, whereas the segment consisting of residues 120–134 contains deletions with respect to the amino acid sequences of eAspAT and mAspATs. The previous eTyrAT model [8] based on the mAspAT crystal structure showed remarkable similarity to it (the r.m.s. deviation for all equivalent C_α atoms is only 0.35 Å). It may well be that this close agreement is due to the simplified model building procedure. The low r.m.s. deviation of 0.47 Å obtained for the comparison between their modelled eAspAT structure [8] and the crystal structure of mitochondrial AspAT indirectly suggests this since this r.m.s. deviation is in fact much larger (1.24 Å) if the relevant experimentally determined structures are compared. A number of residues from the N-terminal portion of the small domain (residues 15–46) in the eTyrAT model form together with side chains from the neighbouring subunit an extensive hydrophobic patch around the active site entry. This area of hydrophobic contact might be responsible for stabilizing the closed conformation of eTyrAT. Kinetic studies [20] and X-ray crystallographic analyses of V39L eAspAT and wild type eAspAT, provide experimental evidence to support this notion. The loop consisting of residues 27–30 is highly flexible in eAspAT as indicated by a temperature factor analysis of eAspAT crystal structures and by the fact that the electron density within this region is weak. Thus, the quite large deviations between the model of eTyrAT and the eAspAT crystal structure in this region are plausible.

3.2. *Active site*

In the active site, which can be subdivided into a cofactor-binding and a substrate-binding region, most of the catalytically important residues of AspATs are

†The usual convention for sequence numbering based on the (longest) pig cytosolic AspAT sequence was followed [2]

Table I

Important variant residues[a] in the active site region of AspATs and TyrATs

Position	eTyrAT	ratTyrAT	eAspAT	cAspAT	mAspAT
18	Leu	Arg	Leu	Phe	Leu
37	Ile	Ile	Ile	Val	Val
39	Leu	Asp	Val	Ala	Ala
69	Leu	–[b]	Asn	Glu	Glu
107	Gly	Thr	Gly	Gly	Ser
141	Glu	Ser	Pro	Glu	Gly
142	Asn	Leu	Asn	Asn	Asn
257	Ser	Ala	Ser	Ser	Ala
293*	Arg	Ile	Ala	Thr	Pro
297*	Ser	Cys	Asn	Asn	Asn

[a] Conserved residues were collated in [5] and are not listed here.
[b] Deletion [5].

conserved in eTyrAT [20]. Amino acid substitutions found in the active site regions of related transaminases are collated in Table I. The cofactor binding site in TyrAT consists of residues mainly from the large domain but also includes Tyr70* (an asterisk signifies a residue from the neighbouring subunit). The hydrogen bonding network around the coenzyme pyridine ring and the 5′-phosphate moiety in the present eTyrAT model is essentially identical to that determined crystallographically for AspAT's (Fig. 2A).

The substrate binding pocket (Fig. 2B) is slightly less conserved, as expected from the different substrate specificities. The substitutions found in the vicinity of arginine 292*, the main determinant of the AspAT substrate specificity, are also listed in Table I. This region includes residues 18, 37, 39, 141, 142, 293* and 297*. The two residues following Trp^{140}, i.e. Glu^{141} and Asn^{142}, both form hydrogen bonds with main-chain and side-chain atoms of Arg^{292*} (not shown). This ensures that the guanidinium group does not approach the side chain of tyrosine too closely. The guanidinium group is further anchored by a salt bridge to Asp^{15} (not shown). All these interactions allow for one of the hydrogen atoms of the Arg^{292*} guanidinium group to point towards the substrate's π electron system, forming favourable geometry for a further attractive interaction [21]. In the present eTyrAT model the β-hydroxyl group of Ser^{297*}, which is an asparagine in all AspATs known to date, is within hydrogen bonding distance (3.2 Å) of the phenolic hydroxyl group of the tyrosine substrate. The serine β-hydroxyl group thus seems to serve as hydrogen bond partner for the phenolic hydroxyl group of the substrate, most likely directly, or perhaps indirectly via a water molecule. The point mutation Ser^{297*} to Asn presumably would hinder productive binding of aromatic substrates to eTyrAT by reducing the size of the substrate binding pocket. Studies of the mutant N297S in eAspAT are being planned to investigate the importance of this residue in the transamination of aromatic

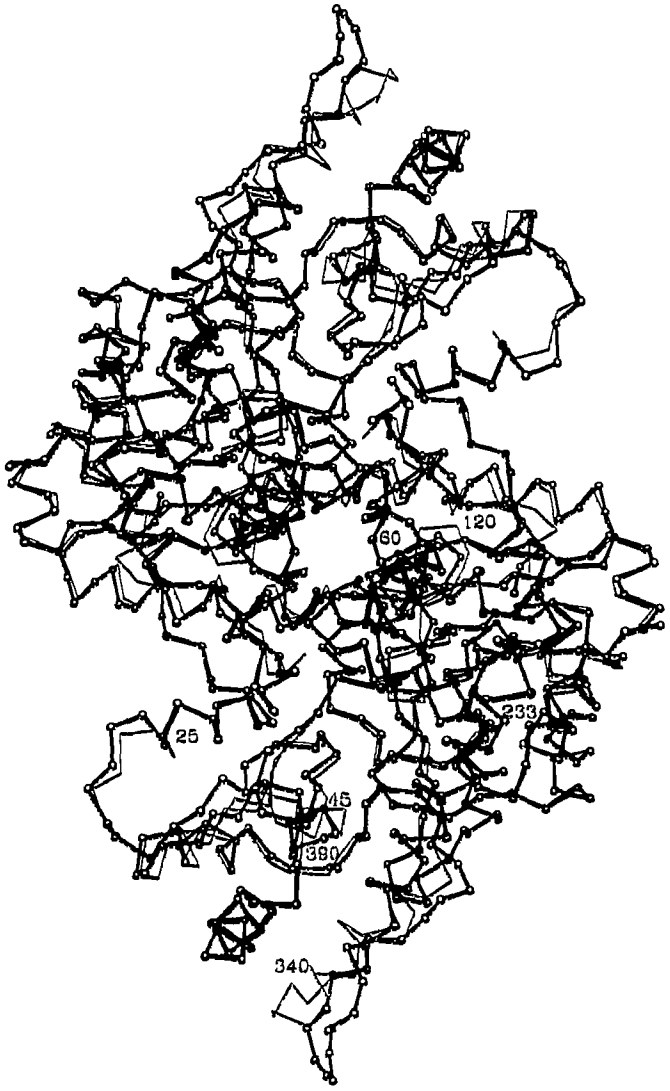

Fig. 1. Superposition of α-carbon models of eTyrAT and eAspAT. Balls and sticks: eTyrAT model; thin lines: V39L mutant eAspAT crystal structure. Only residues in one subunit of the dimer are numbered.

amino acids. The present study suggests that binding of aromatic substrate side chains to TyrAT is achieved through a complex interaction pattern unlike that involving bidentate hydrogen bonds and salt bridges found in AspATs for the interactions of the distal carboxylates in dicarboxylate substrates with Arg^{292*}. From the studies of the V39L mutant of eAspAT [7,8] which was expected to shift the substrate specificity towards aromatic substrates it is clear that this residue alone is not responsible for changing the enzyme selectivity. The distribution of charged groups around Arg^{292*} in TyrAT differs substantially from that in AspATs. Thus, it would be expected that the negative charges of Asp^{15} and Glu^{141}, which are not present in the eAspAT, exert repulsive forces on the negatively

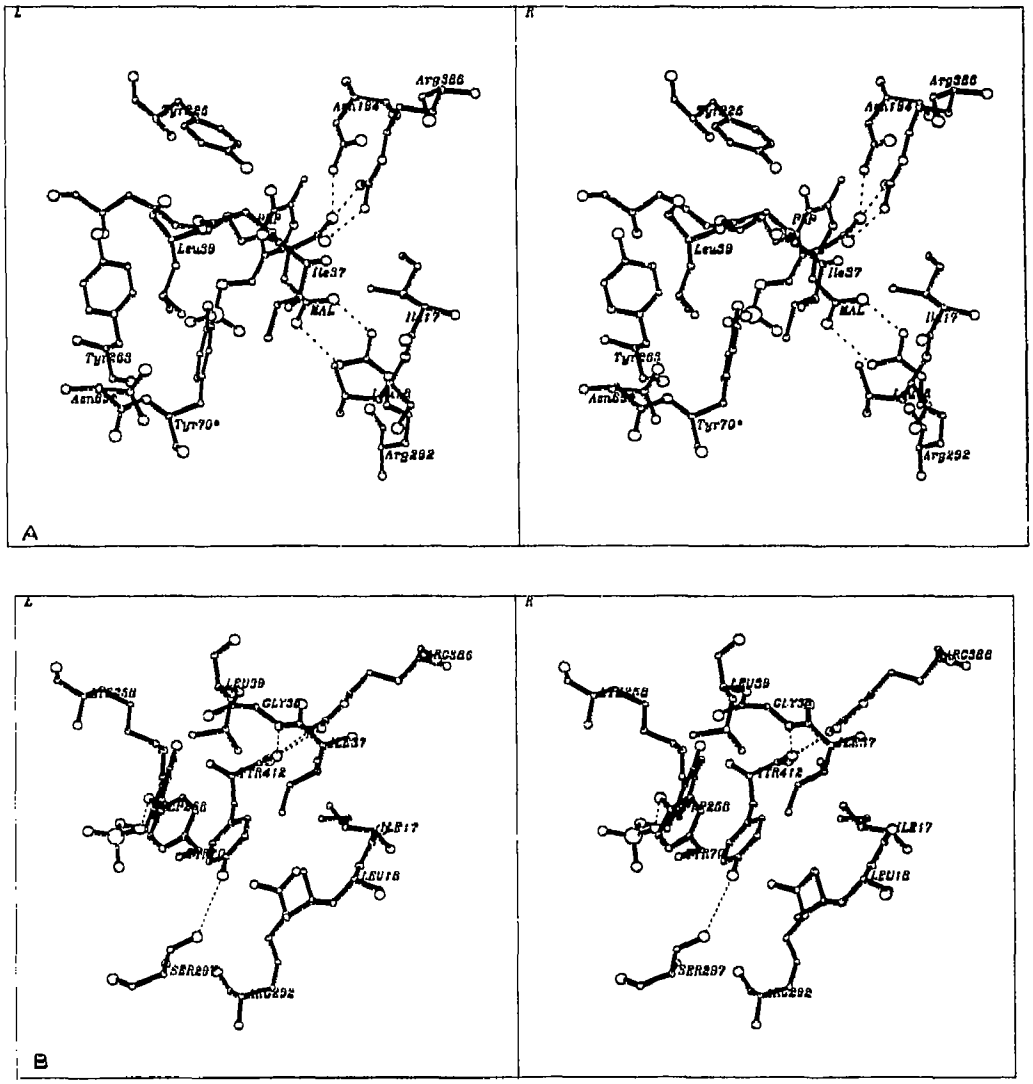

Fig. 2. Partial active sites of V39L eAspAT crystal and eTyrAT model structures. (A) V39L eAspAT structure. Residues Ile[17], Val[18], Ile[37], Leu[39] and Asn[69]* form a hydrophobic lid above the substrate binding pocket, shielding it from bulk solvent. The van der Waals' contacts between Leu[39] and residues Asn[69]*, Tyr[70]* and Tyr[263] strengthen the subunit–subunit interactions and stabilize the closed conformation. The inhibitor maleate, mimicking the Michaelis complex with aspartate forms double hydrogen bond/ion pair interactions to the guanidinium groups of both Arg[386] and Arg[292]*. Hydrogen bonds are indicated by dashed lines. (B) eTyrAT model. The substitution of Asn[297] (fully conserved in AspATs) by serine gives rise to an enlarged binding pocket in TyrAT and a different binding mode for aromatic substrates. Since Ile[17], Arg[386], Tyr[70]*, Arg[292]* are all conserved in the active sites of eAspAT and eTyrAT (Table I), Ser[297]* is likely to be responsible for the reduced Michaelis constants, i.e. high affinity binding of aromatic substrates as compared to eAspAT. The catalytic activity of eTyrAT towards dicarboxylic acid substrates remains unchanged as Arg[292]* is still available for tight binding to the distal carboxylate group.

charged distal carboxylate groups of substrates like aspartate or glutamate and, therefore, such substrates might conceivably bind less tightly to this active site. Productive binding of dicarboxylic acid substrates to eTyrAT would probably also involve dissociation of the salt bridge between Arg[292]* and Glu[141]. The latter would have to be rotated out of the active site towards the solvent. However, cytosolic AspATs also have a glutamate residue in position 141. The charge distribution in these enzymes differs from that in the mitochondrial or *E. coli* enzymes in that valine instead of aspartate is found in position 15 suggesting that in the cytosolic AspATs only Glu[141] serves as additional charge anchor compensating the flexible extended side chain of Arg[292]*. Experimental data on binding of dicarboxylic acid substrates to various AspAT's and TyrAT's [8,9] indicate, however, that both enzymes bind these substrates approximately equally well. Thus, it would appear that either the substrate specificity is not sensitive to changes in the local electrostatic environment introduced by the mutations in position 15 and 141, or that the proposed TyrAT structure is not adequate. Prelimi-

nary results of further work which is being carried out in this laboratory using an electrostatic potential approach and based on the experimental and model structures discussed in this paper substantiate the first notion and further support the proposed TyrAT model structure.

Acknowledgements: This work was supported in part by the Swiss National Science Foundation (Grants 31-25712.88 and 31-26261.89). We would like to thank Drs. R. Pauptit and M.D. Toney for critically reading the manuscript and very useful suggestions. The support of the University Computer Center, Basel and the Supercomputing Center ETH, Zürich is gratefully acknowledged.

REFERENCES

[1] Braunstein, A.E. (1973) In: The Enzymes (Boyer, P.D. Ed.) Vol. 9, 3rd ed., Academic Press, New York, pp. 379–481.
[2] Christen, P. and Metzler, D.E., Eds. (1985) Transaminases, Wiley, New York.
[3] Kirsch, J.F., Eichele, G., Ford, G.C., Vincent, M.G., Jansonius, J.N., Gehring, H. and Christen, P. (1984) J. Mol. Biol. 174, 497–525.
[4] Jansonius, J.N. and Vincent, M.G. (1987) In: Biological Macromolecules and Assemblies (Jurnak, F.A. and McPherson, A., Eds.) vol. 3, John Wiley, New York, pp. 187–285.
[5] Mehta, P.K., Hale, T.I. and Christen, P. (1989) Eur. J. Biochem. 186, 249–253.
[6] Fotheringham, I., Dacey, S., Taylor, P., Smith, T., Hunter, M., Finlay, M., Primrose, S., Parker, D. and Edwards, M. (1986) Biochem. J. 234, 593–604.
[7] Köhler, E. (1990) Ph.D. Thesis, University of Basel.
[8] Seville, M., Vincent, M.G. and Hahn, K. (1988) Biochemistry 27, 8344–8349.
[9] Jardetzky, T.S. and Seville, M. (1988) Biochemistry, 27, 6758–6763.
[10] Jäger, J., Köhler, E., Tucker, P., Sauder, U., Housley-Markovic, Z., Fotheringham, I., Edwards, M., Hunter, M., Kirschner, K. and Jansonius, J.N. (1989) J. Mol. Biol. 209, 499–501.
[11] Jäger, J. (1991) Ph.D. Thesis, University of Basel.
[12] Jäger, J. et al. (1991) In: Proceedings of the 8th International Symposium on Vitamin B_6 and Carboxyl Catalysis, Osaka, 1990, Pergamon Press, Oxford, 117–119.
[13] Brünger, A.T. (1990) X-PLOR Manual, Version 2.1, Yale University.
[14] Genetics Computer Group (GCG), University of Wisconsin, Sequence Analysis Software Package, Version 6.2 (1990).
[15] Smith and Waterman (1981) Adv. Appl. Math. 2, 482–489.
[16] Chou, H. and Fasman, G. (1978) Adv. Enzymol. 47, 45–148.
[17] Garnier, J., Osguthorpe, D.J., Robson, B. (1978) J. Mol. Biol. 120, 97–120.
[18] Van Gunsteren, W.F. and Berendsen, H.J. (1987) Groningen Molecular Simulation (GROMOS) Library Manual, BIOMOS, Nijenborgh, Groningen, The Netherlands.
[19] Solmajer, T. and Mehler, E.L. (1991) Prot. Eng. 4, 911–917.
[20] Hayashi, H., Kuramitsu, S. and Kagamiyama, H. (1991) J. Biochem. (Tokyo) 109, 699–704.
[21] Levitt, M. and Perutz, M.F. (1988) J. Mol. Biol. 201, 751–754.